Signal Transduction:

Histidine-containing Phosphotransfer Protein-B (HptB) Regulates Swarming Motility through Partner-switching System in *Pseudomonas aeruginosa* PAO1 Strain

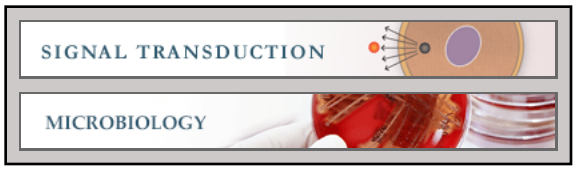

Manish Bhuwan, Hui-Ju Lee, Hwei-Ling Peng and Hwan-You Chang

J. Biol. Chem. 2012, 287:1903-1914.
doi: 10.1074/jbc.M111.256586 originally published online November 29, 2011

THE JOURNAL OF BIOLOGICAL CHEMISTRY VOL. 287, NO. 3, pp. 1903–1914, January 13, 2012

Histidine-containing Phosphotransfer Protein-B (HptB) Regulates Swarming Motility through Partner-switching System in *Pseudomonas aeruginosa* PAO1 Strain[S]

Received for publication, May 1, 2011, and in revised form, November 28, 2011 Published, JBC Papers in Press, November 29, 2011, DOI 10.1074/jbc.M111.256586

Manish Bhuwan[‡], Hui-Ju Lee[§], Hwei-Ling Peng[§], and Hwan-You Chang[‡1]

From the [‡]Institute of Molecular Medicine, National Tsing Hua University and [§]Department of Biological Science and Technology, National Chiao Tung University, Hsin Chu 300, Taiwan

Background: This study investigates how histidine phosphotransfer protein-B (HptB) regulates *Pseudomonas aeruginosa* swarming.
Results: HptB regulates the protein phosphatase activity of PA3346, which in turn controls the flagellar gene expression through interaction with PA3347.
Conclusion: Our results reveal a partner-switching mechanism regulating the σ^{28}-dependent motility genes.
Significance: The interplay between a two-component system and σ^{28} has been established.

The histidine-containing phosphotransfer protein-B (HptB; PA3345) is an intermediate protein involved in transferring a phosphoryl group from multiple sensor kinases to the response regulator PA3346 in *Pseudomonas aeruginosa* PAO1. The objective of this study was to elucidate the biological significance of the HptB-PA3346 interaction and the regulatory mechanisms thereafter. The transcription profiling analysis of an *hptB* knock-out mutant showed that the expression of a number of motility-related genes was altered consistent with the non-swarming phenotype observed for the mutant. Domain analysis indicated that the PA3346 C-terminal region (PA3346C) exhibits ~30% identity with the anti-σ factor SpoIIAB of *Bacillus subtilis*. The presence of Ser/Thr protein kinase activity targeting an anti-σ antagonist, PA3347, at Ser-56 was confirmed in PA3346C using an *in vitro* phosphorelay assay. Furthermore, PA3346C and the anti-σ^{28} factor FlgM were found to interact with PA3347 individually both *in vivo* and *in vitro*. FlgM displaced PA3346C in binding of PA3347 and was then competitively displaced by σ^{28} from the PA3347-FlgM complex, forming a phosphorylation-dependent partner-switching system. The significance of PA3347 phosphorylation in linking the partner-switching system and swarming motility was established by analyzing the swarming phenotype of the *PA3347* knock-out mutant and its complement strains.

Two-component signal transduction systems are commonly utilized by bacteria to sense and respond to environmental alterations. A two-component system typically comprises a sensor histidine kinase and a response regulator. After receiving stimuli, the sensors undergo autophosphorylation at a conserved histidine residue before transferring the phosphate group to a response regulator either directly or through an intermediate such as a histidine-containing phosphotransfer (Hpt)[2] protein (1, 2). The response regulators are typically multidomain proteins that comprise a conserved receiver and a variable effector domain. The interdomain communication between the regulatory and effector domains of a response regulator shows significant diversity. Removal of the receiver domain may inhibit or constitutively activate the effector domain (3, 4). A more intricate role for response regulators was found in PhyR, which combines a receiver domain with an N-terminal domain that is extremely similar to the σ^{E} subunit of RNA polymerase. Unlike other DNA-binding transcriptional regulators, PhyR acts through protein-protein interaction in a partner-switching mechanism where the σ^{E} domain of PhyR binds to the anti-σ factor NepR. As a result, the original σ factor σ^{EcfG} is free to transcribe stress-related genes (5).

Partner-switching regulatory systems typically comprise anti-anti-σ, anti-σ, and σ factors. Dephosphorylation of the anti-anti-σ factor by a Ser/Thr protein phosphatase enables its direct interaction with the anti-σ factor, rendering it unavailable to bind to the σ factor. The σ factor is then free to transcribe the downstream genes (6, 7). Once the anti-anti-σ is phosphorylated by the Ser/Thr protein kinase activity of the anti-σ factor, it dissociates from the anti-σ factor, which is then free to bind to the σ factor, consequently inhibiting the downstream gene expression. Such a signaling paradigm was first observed in *Bacillus subtilis* SpoIIE-SpoIIAB-SpoIIAA, which forms partner switchers when regulating sporulation-related σ^{F} (8). The other example is *Bordetella bronchiseptica* BtrU-BtrW-BtrV, which is responsible for regulating a Type III secretion system (9).

Pseudomonas aeruginosa is a Gram-negative, motile bacterium and an opportunistic pathogen known to be the leading cause of numerous acute and chronic nosocomial infections. Our previous studies of *P. aeruginosa* two-component regulatory systems revealed that following activation by environmental stresses multiple sensor kinases (PA1611, PA1976, PA2824,

[S] This article contains supplemental Figs. S1–S3, Tables S1–S3, and Videos S1 and S2.

[1] To whom correspondence should be addressed. Tel.: 886-3-574-2909; Fax: 886-3-574-2910; E-mail: hychang@life.nthu.edu.tw.

[2] The abbreviations used are: Hpt, histidine-containing phosphotransfer protein; PA3346C, PA3346 C-terminal region; BiFC, bimolecular fluorescence complementation; NGFP, N-terminal GFP; CGFP, C-terminal GFP.

TABLE 1
Bacterial strains and plasmids used in this study

Strains and plasmids	Description	Source/Ref.
Strains		
E. coli		
BL21(DE3)	F^- *ompT gal dcm lon hsdS*$_B$(r_B^- m_B^-) λ(DE3) [*lacI lacUV5*-T7 gene *1 ind1 sam7 nin5*]	Invitrogen
XL-1 Blue	*endA1 gyrA96*(*nal*^{R}) *thi-1 recA1 relA1 lac glnV44 F'*[::*Tn*10 *proAB*$^+$ *lacI*^{q} Δ(*lacZ*)*M15*] *hsdR17*(r_K^- m_K^+)	Stratagene
P. aeruginosa		
PAO1	Non-mucoid wild-type strain	Laboratory stock
MPA45	PAO1Δ*hptB*	11
MJL46	PAO1Δ*PA3346*	12
MJL47	PAO1Δ*PA3347*	12
Plasmids		
pGEX-5X-1	Ap^r, GST tag protein expression vector	Amersham Biosciences
pET30a	Km^r, His tag protein expression vector	Novagen
pGEX47	Ap^r, a fragment containing entire *PA3347* coding region cloned into pGEX-5X-1	12
pE3347-S56A	Ap^r, a fragment containing entire *PA3347-S56A* coding region cloned into pGEX-5X-1	12
pMBH3051	Km^r, a fragment containing entire *flgM* coding region cloned into pET30a	This study
pET11a-link-NGFP	Ap^r, plasmid vector designed for fusion of a target protein to the N-terminal fragment of GFP (1–157)	26, 27
pMRBAD-Z-CGFP	Km^r, plasmid vector that expresses a fusion of an antiparallel leucine zipper peptide to CGFP	26, 27
pET11a-Z-NGFP	Ap^r, plasmid vector that expresses a fusion of an antiparallel leucine zipper peptide to NGFP	26, 27
pMRBAD-link-CGFP	Km^r, plasmid vector designed for fusion of a target protein to the C-terminal fragment of GFP (158–238)	26, 27
pNBIFC3347	Ap^r, a fragment containing entire *PA3347* coding region cloned into pET11a-link-NGFP with three additional linkers	This study
pNBIFC3347M	Ap^r, a fragment containing entire *PA3347-S56A* coding region cloned into pET11a-link-NGFP with three additional linkers	This study
pCBIFC3351	Km^r, a fragment containing entire *flgM* coding region cloned into pMRBAD-link-CGFP	This study
pHLBIFC46	Km^r, a fragment containing residues 1224–1716 coding region cloned into pMRBAD-link-CGFP	This study
pHL34	Km^r, a fragment containing residues 1222–1713 of *PA3346* coding region cloned into pET30a	This study
pMBH551	Ap^r, a fragment containing entire *flgM* coding region in pGEX-5X-1	This study
pMBH3028	Km^r, a fragment containing entire *fliA* coding region in pET30a	This study
pMBH10047	Ap^r, a fragment containing entire *PA3347* region in pET100	This study
pHL40	Km^r, a fragment containing entire *fliA* coding region in pET30a	This study
pMMB66EH	Ap^r; broad host range expression vector	52
pMMB47	Ap^r, a fragment containing entire *PA3347* in pMMB66EH	12
pMMB47S56A	Ap^r, a fragment containing *PA3347-S56A* in pMMB66EH	This study
pMMB47S56D	Ap^r, a fragment containing *PA3347-S56D* in pMMB66EH	This study

and RetS) transfer a phosphoryl group to HptB, which then relays the signal to the response regulator PA3346. The phosphorylation on the PA3346 N-terminal receiver domain increases its Ser protein phosphatase activity, leading to dephosphorylation of the potential anti-anti-σ factor PA3347. Although the target phosphorylation site of PA3347 was shown to be Ser-56, the corresponding Ser protein kinase and anti-σ factors remain elusive. The isogenic *hptB* deletion mutant is defective in swarming, whereas the *PA3346* or *PA3347* mutant showed increased swarming compared with swarming and other characteristics for the involvement of motility genes in *P. aeruginosa* PAO1 (10–12).

According to recent information from the *Pseudomonas* genome database and the *P. aeruginosa* Community Annotation Project (PseudoCAP), ~50 flagellum and chemotaxis genes are present in the *P. aeruginosa* PAO1 genome (13, 14). The checkpoint for flagellum biogenesis is complex, requiring at least two σ factors, RpoN (σ^{54}) (15) and FliA (σ^{28}) (16). The direct interaction of FliA and the anti-σ factor FlgM in *P. aeruginosa* was demonstrated using the yeast two-hybrid system, which revealed their role in regulating flagellar biogenesis using a post-translational mechanism (17).

The *P. aeruginosa* flagellum plays a critical role in virulence as shown by several animal models where the bacteria with flagella were more invasive than flagellum-deficient strains (18). The strain with a deletion at *fliC*, which codes for the major flagellin in *P. aeruginosa*, showed a loss of virulence in a pulmonary infection model. These results suggest that the flagellum plays a key role in the *P. aeruginosa* invasion of epithelial cells (19). Recently, Bordi *et al.* (20) demonstrated that the HptB signaling pathway is linked to the regulation of the GacA/GacS two-component system by down-regulating the expression of *rsmY*, a small RNA. Because *rsmY* is a known regulator of the Type VI secretion system (21), HptB may also negatively regulate protein secretion.

The objective of this study was to explain the regulatory mechanism of HptB-PA3346-PA3347. The microarray analysis of an *hptB* mutant revealed that a number of the FliA-dependent motility genes were down-regulated, and these results were validated via real time PCR. We also demonstrate that the PA3346 C-terminal region (PA3346C) is a novel Ser/Thr protein kinase that phosphorylates and thereby regulates the activity of PA3347. Our results demonstrate that PA3347 interacts with FlgM and PA3346C in a competitive manner. Overall, these findings indicate that HptB, PA3346, PA3347, FlgM, and FliA are organized into a phosphorylation-dependent partner-switching system that regulates bacterial swarming.

EXPERIMENTAL PROCEDURES

Bacterial Strains, Plasmids, and Primers—The bacterial strains and plasmids used in this study are listed in Table 1. The primers used are listed in supplemental Table S1.

Microarray Analysis for Transcriptional Profiling of P. aeruginosa PAO1 and hptB Mutant MPA45—*P. aeruginosa* PAO1 and *hptB* mutant strain MPA45 were cultured on swarming plates for 36 h at 30 °C. Bacteria were collected from the edge of swarming bacterial colonies, and the RNA was extracted using a Qiagen RNeasy Midi kit (Qiagen, German-

town, MD). Residual genomic DNA was removed using RQ1 DNase (Promega, Madison, WI). Approximately 10 μg of the RNA from both *P. aeruginosa* PAO1 and the *htpB* knock-out mutant MPA45 was reverse transcribed into cDNA using Superscript II reverse transcriptase (Invitrogen). The resulting cDNA was purified using a Qiagen PCR purification kit and tagged with biotin using the GeneChip® DNA labeling reagent (Affymetrix) according to the manufacturer's instructions. The labeled cDNA was used to hybridize the Affymetrix GeneChip. Data were normalized by Linear Models for Microarray Data (22), and differential gene expression tables were generated.

Real Time Quantitative PCR Analysis—The same total RNA source for *P. aeruginosa* PAO1 and MPA45 used in the microarray gene expression profile was used in the validation experiment through real time quantitative PCR analysis. Approximately 1.5 μg of RNA was reverse transcribed into cDNA using Superscript II reverse transcriptase (Invitrogen). For real time PCR quantification using the cDNAs of *P. aeruginosa* PAO1 and MPA45, primer sets specific for genes *fliC*, *fliD*, *fliM*, *flgM*, *PA4915*, and *cheY* were designed using the Primer Express software under the factory default settings. Two housekeeping genes, *rpoD* and *proC*, were used as an internal control of gene expression, and the mean of the *proC* and *rpoD* expression levels in the sample was used as the normalization factor (23). All primers were tested for the absence of nonspecific bands or primer dimer formation prior to real time PCR analysis. Real time PCR was performed with SYBR® Green Master Mix and analyzed using the Fast 7500 Real-Time PCR system (Applied Biosystems, Foster City, CA). The data analyses for real time PCR were performed using the Applied Biosystems Sequence Detection System software, version 1.4. A comparative Ct method was applied to quantify the expression levels. All genes were examined in duplicate. The quantitative data of mRNA expression for *P. aeruginosa* PAO1 and MPA45 obtained from two independent experiments were calculated using the $2^{-\Delta\Delta Ct}$ method (24). Similarly, the cDNAs of *P. aeruginosa* PAO1 and the *PA3347* deletion mutant MJL47 were used to quantify *fliA* and *flgM* using an appropriate set of primers.

Bioinformatics Analysis—Proteins resembling PA3346 were detected in the NCBI database using the protein BLAST search tool. A comparison and an alignment of these homologous protein sequences were performed using Vector NTI® (Invitrogen) to identify the conserved amino acid residues. Identification of restriction sites and open reading frame predictions were also conducted using Vector NTI.

Construction of Plasmids—The restriction endonucleases and DNA-modifying enzymes were purchased from New England Biolabs (Ipswich, MA). *P. aeruginosa* PAO1 genomic DNA was purified with the Wizard Genomic DNA Purification kit (Promega) and used as the template for PCR amplification. The PCR product for the C-terminal region of PA3346 (from nucleotide position 1222 to 1713) and *flgM* was digested with restriction enzymes NdeI and NotI and ligated directionally into the expression vector pET30a (Novagen, Madison, WI) to generate plasmids pHL34 and pMBH3051, respectively. Similarly, the PCR product of *fliA* was digested with NdeI and HindIII and ligated into pET30a to yield the plasmid pHL40. The PCR product of *PA3347* was ligated into pET100 (Invitrogen), providing the clone pMBH10047. In another set of experiments, the PCR product of *flgM* was digested with EcoRI and XhoI and ligated directionally into the expression vector pGEX-5X-1 (Amersham Biosciences), resulting in pMBH551. For the bimolecular fluorescence complementation (BiFC) assay, the PCR products of *PA3347* and *PA3347-S56A* were digested with a restriction enzyme and then ligated into the pET11a-link-NGFP vector at the XhoI and BamHI restriction enzyme sites, resulting in pNBIFC3347 and pNBIFC3347M, respectively. Similarly, the PCR products of *flgM* and *PA3346C* were digested using restriction enzymes NcoI and AatII and fused into the pMRBAD-link-CGFP vector, resulting in clones of pCBIFC3351 and pHLBIFC46, respectively. Nucleotide sequencing was performed to verify whether the sequences were correct and in-frame in these plasmids.

Expression and Purification of Recombinant Proteins—The *Escherichia coli* BL21(DE3) cells were transformed with the pET-based *flgM*, *fliA*, and *PA3346C* clones separately, and gene expression was induced using isopropyl β-D-thiogalactopyranoside at a final concentration of 0.1 mM with a constant shaking rate of 150 rpm at 20 °C for 16 h. The cells were collected by centrifugation, resuspended in a lysis buffer (20 mM Tris-HCl, pH 8.0, 1 mM phenylmethylsulfonyl fluoride, 500 mM NaCl), and disrupted on ice by ultrasonication. After centrifugation at 14,000 rpm at 4 °C for 20 min to remove debris, the clarified supernatant was loaded onto a nickel-charged resin (Ni-Sepharose™ High Performance, Amersham Biosciences), and the proteins retained in the column were eluted using the elution buffer (50 mM sodium phosphate, 300 mM NaCl, 500 mM imidazole, pH 8.0). Similarly, glutathione *S*-transferase (GST)-tagged PA3347, PA3347-S56A, FlgM, and glutathione *S*-transferase recombinant proteins were affinity-purified on glutathione-Sepharose 4 Fast Flow resin (Amersham Biosciences) separately using the GST elution buffer (50 mM Tris-HCl, pH 8.0, 20 mM glutathione). The purified proteins were dialyzed against PBS (137 mM NaCl, 2.7 mM KCl, 10 mM Na_2HPO_4, 2 mM KH_2PO_4, 50% glycerol, pH 7.4), and the concentration of these proteins was determined via the Bradford method using a Bio-Rad kit.

In Vitro Phosphorylation Assay and Tandem Mass Spectrometric Analysis—To detect the Ser protein kinase activity, both PA3347 and PA3347-S56A, a non-phosphorylatable amino acid substitution variant of PA3347, were incubated individually with PA3346C in phosphorylation buffer (50 mM Tris-HCl, 200 mM KCl, 10 mM $MgCl_2$, 1 mM EDTA, 1 mM dithiothreitol) and 1 μCi of [γ-^{32}P]ATP at 37 °C for 1 h. The reactions were quenched by adding the same volume of the SDS-PAGE loading dye (50 mM Tris-HCl, pH 6.8, 100 mM dithiothreitol, 2% sodium dodecyl sulfate, 0.1% bromphenol blue, 10% glycerol, 10% β-mercaptoethanol) and heated at 95 °C for 10 min. The phosphorylation patterns were detected using autoradiography.

In vitro phosphorylation for mass spectrometer analysis was performed as described above except that [γ-^{32}P]ATP was replaced with 5 mM unlabeled ATP. The eluted sample was further resolved by SDS-PAGE. In-gel digestion was performed as described previously (25) with the following modifications: destaining was achieved by washing the gel twice with 20 mM

NH_4HCO_3, acetonitrile (1:1 mixture) for 15 min at room temperature, and reduction was performed using 10 mM dithiothreitol in 20 mM NH_4HCO_3 for 15 min at 56 °C. Alkylation was performed using 55 mM iodoacetamide in 20 mM NH_4HCO_3 for 20 min in darkness at room temperature. For proteolytic digestion, the gel was treated overnight at 37 °C with 20 μg of sequencing grade trypsin (Promega). The digested sample was sonicated for 10 min in the presence of 1% trifluoroacetic acid, and the supernatant was pooled and subjected to MALDI-TOF mass spectrometer analysis.

Kinetics of PA3347 Phosphorylation—Four different concentrations (0.25–2.0 μM) of PA3347 were incubated with PA3346C (1 μM) in the presence of 0.1 mM ATP and 10 mM $MgSO_4$ in a 30-μl volume at 37 °C for 7 min. During this period of time, the PA3347 phosphorylation levels were linear with regard to time. The phosphorylation assay was terminated by adding an equal volume of the SDS loading buffer and boiled for 10 min. The protein was resolved using polyacrylamide gel electrophoresis and transferred to a polyvinylidene fluoride (PVDF) membrane (Amersham Biosciences). The membrane was probed with a phosphoserine-specific mouse monoclonal antibody (Qiagen) followed by a horseradish peroxidase-conjugated secondary antibody. The band was visualized using a NovaRED™ Substrate kit (Vector Laboratories, Burlingame, CA). The phosphorylation intensity was determined by quantifying the immunoblot using ImageJ software, and kinetics analysis was performed using the GraphPad Prism® software.

GST Pulldown Assay—The recombinant proteins for testing protein-protein interaction were incubated with 500 μl of a 50% slurry of glutathione-agarose beads in PBS for 2 h at 4 °C either in the absence or presence of 2 mM ADP and 2 mM $MgSO_4$. The reaction mixture was then centrifuged at 3,000 rpm for 5 min, the precipitated glutathione beads were washed twice with PBS, the protein complex was eluted with the GST elution buffer, and the eluted fraction was concentrated using Amicon Ultra (Millipore, Billerica, MA). The proteins present in the eluted fractions were resolved on a polyacrylamide gel and then transferred onto a PVDF membrane. The membrane was incubated sequentially with a monoclonal antibody against His tag (Merck KGaA) and a horseradish peroxidase-conjugated secondary antibody (Jackson ImmunoResearch Laboratories, West Grove, PA). Finally, the target proteins were identified using a NovaRED Substrate kit (Vector Laboratories).

BiFC Assay—The BiFC assay was performed as described previously (26, 27) with slight modifications. The positive control plasmid pair was pET11a-Z-NGFP and pMRBAD-Z-CGFP encoding the green fluorescence protein fused with one of the antiparallel leucine zipper tags, respectively. The negative control was the cells harboring pET11a-link-NGFP and pMRBAD-link-CGFP. The interacting partners were introduced into *E. coli* BL21(DE3), and the transformants were cultured on Luria-Bertani agar containing 50 μg/ml ampicillin, 35 μg/ml kanamycin, 0.1 mM isopropyl β-D-thiogalactopyranoside, and 0.05% arabinose at 20 °C for 72 h. The cells were examined for the presence of green fluorescence by an Olympus BX-51 epifluorescence upright microscope. The images were analyzed using a digital camera and SPOT Advanced Plus Imaging Software (version 4.6).

Antibody Production and Co-immunoprecipitation—Recombinant GST-PA3347 protein was used as an immunogen to raise rabbit polyclonal antisera for detecting both PA3347 and PA3347-S56A. The co-immunoprecipitation was performed as described previously (28, 29). Protein A-Sepharose beads (125 μl; Amersham Biosciences) were incubated overnight at 4 °C with 50 μg of rabbit polyclonal PA3347 antibody in 125 μl of Pierce ImmunoPure Ag/Ab binding buffer (Thermo-Fisher Scientific Inc., Rockford, IL). For the co-immunoprecipitation of PA3347 with His_6-FlgM, beads were incubated with 500 μl of the whole cell lysates from ~10^9 cfu of PAO1 and 200 μg of His_6-FlgM at 4 °C overnight under constant agitation. For the co-immunoprecipitation of GST-PA3347-S56A with His_6-FlgM, beads were incubated with 500 μl of the whole cell lysates of *E. coli* expressing GST-PA3347-S56A from ~10^9 cfu and 200 μg of His_6-FlgM. In both cases, whole cell lysates alone and His_6-FlgM alone were used as negative controls. The co-immunoprecipitation of PA3347 with His_6-PA3346C was similarly performed. The beads were washed with PBS and boiled in SDS loading dye for 10 min. Western blotting was conducted using the mouse monoclonal anti-His_6 antibody (1:2,500) as the primary antibody and the goat anti-mouse IgG antibody conjugated to HRP (1:10,000) as the secondary antibody.

Competitive Interaction Using GST Pulldown Assay—To investigate the binding activity of PA3346C *versus* FlgM on PA3347 in the presence of ATP or ADP, a competition assay was performed as described previously (30) with slight modifications. A constant concentration of PA3347 (25 μg/ml) bound to FlgM (30 μg/ml) was incubated on 100 μl of a 50% GST bead slurry in six separate tubes. Following 2 h of mixing, 2 mM ADP and 2 mM $MgSO_4$ were added to three microcentrifuge tubes with increasing concentrations of PA3346C (0, 10, and 20 μg/ml). Meanwhile, in three other tubes, 2 mM ATP was added instead of ADP and then incubated for 2 h. In a reciprocal experiment, a constant concentration of PA3347 was bound to PA3346C and incubated with increasing concentrations of FlgM (0, 15, and 30 μg/ml) in the presence of either ATP or ADP. In this study, GST was used as a negative control.

Similarly, to demonstrate that increasing concentrations of FliA (0, 20, and 100 μg/ml) compete to bind with FlgM (30 μg/ml) in a complex comprising PA3347 (30 μg/ml), a competition assay was performed. The GST beads carrying the interacting proteins were washed with PBS extensively and then eluted with the GST elution buffer. The proteins present in the eluents were resolved using SDS-polyacrylamide gel electrophoresis.

Analysis of Bacterial Swarming—A swarming assay for *P. aeruginosa* PAO1 and *P. aeruginosa* PA3347 mutant MJL47 was performed as reported previously (12). Briefly, the swarming assay medium comprises an M8 salt base (50 mM Na_2HPO_4, 25 mM KH_2PO_4, 4 mM NaCl) supplemented with 0.5% Bacto agar, 0.02% glucose, and 10 mM glutamic acid. The bacterial strains that required testing were cultured overnight, transferred to the swarming plate using sterile toothpicks, and then incubated at 37 °C for 36 h. The experiment was performed three independent times.

TABLE 2
Comparison of expression levels of selected motility-related genes in hptB mutant determined by real time quantitative PCR (Q-PCR) and microarray

Locus index	Gene name	-Fold change for microarray (*p* value)	-Fold change for Q-PCR (±S.D.)
PA3351	*flgM*	−5.7 (0.070)	−10.2 ± 2.6
PA1092	*fliC*	−3.6 (0.004)	−7.7 ± 0.1
PA1094	*fliD*	−4.5 (0.090)	−28.6 ± 1.0
PA1443	*fliM*	−3.2 (0.010)	−58.6 ± 4.2
PA1456	*cheY*	−3.9 (0.020)	−5.5 ± 0.2
PA4915	NA[a]	−8.7 (0.020)	−6.3 ± 0.5

[a] Not available.

RESULTS

Transcriptional Profiling of P. aeruginosa PAO1 and hptB Mutant—To obtain a more comprehensive picture of the physiological functions of the HptB-PA3346-PA3347 signaling system, a *Pseudomonas* whole genome DNA microarray was used to determine the gene expression profiles of the *hptB* mutant. The results were compared with those of the wild-type PAO1 strain. This study identified 142 genes with a more than 2-fold increase in expression and 235 genes showing at least a 2-fold decrease in expression. The top 20 up- and down-regulated genes are listed in supplemental Tables S2 and S3, respectively. Approximately half of the genes on the list encode a hypothetical protein. Several genes, including *adhA*, *pldA*, *stp1*, and *pilQ* that may be associated with bacterial virulence, were also noted. Among the genes up-regulated in the *hptB* mutant, *adhA* is known to be important in biofilm formation in *P. aeruginosa* (31). This notion is consistent with higher biofilm formation in the *hptB* mutant compared with *P. aeruginosa* (12). The gene *pldA*, which encodes the outer membrane phospholipase D, is known to be involved in chronic pulmonary infections (32). The *stp1* product is a Ser/Thr protein phosphatase belonging to the protein phosphatase 2C family. It might regulate the Type III secretion system or alginate synthesis in *P. aeruginosa* (33). On the down-regulated gene list, the *pilQ* gene product is required for assembly and secretion of the type IV pili (34), which are cell surface organelles mediating adhesion and twitching motility. Finally, the *exsC* gene product acts as an anti-anti-activator for transcription of the Type III secretion system. This is in accordance with the finding that HptB positively controls the Type III secretion system in *P. aeruginosa* (20).

Expression of Certain Flagellum and Chemotaxis Genes Is Down-regulated in hptB Mutant—The reduced expression genes in the *hptB* mutant MPA45 include several motility genes such as *cheY*, which functions as a switch to control the flagellar rotation direction (35), *fliM*, which controls flagellar rotation (36), the flagellar cap protein-encoding gene *fliD*, which participates in the adhesion process (37), and the flagellation protein genes *fliC* and *flgM*. To validate the microarray data, the expression levels of these motility-related genes and *PA4915*, which encodes a hypothetical protein involved in chemotaxis, were measured using quantitative real time PCR. Consistent with the microarray analysis results, these motility-related genes also exhibited reduced expression levels in the quantitative real time PCR assay although with a higher dynamic range of -fold change (Table 2). The discrepancy is not uncommon and may be attributed to many factors such as a difference in data normalization, transcript detection (SYBR Green *versus* CyDyes), and selection of PCR primers and hybridization probes (38).

C-terminal Region of PA3346 Contains Kinase Domain—We have shown previously that HptB (PA3345) can transmit a phosphoryl group from a sensor kinase to PA3346 (12). As a response regulator, the N-terminal region of PA3346 has a signal receiver domain containing a conserved Asp residue. The middle portion of the protein comprises a protein phosphatase 2C domain, which can dephosphorylate PA3347 (12). Further analysis of the C-terminal region of PA3346 using the BLASTP program revealed significant similarity to several confirmed Ser/Thr protein kinases, including *Bacillus stearothermophilus* SpoIIAB (39), *B. subtilis* SpoIIAB (40), *B. subtilis* RsbW (7), and *B. bronchiseptica* BtrW (9) (Fig. 1). The amino acid residues and molecular structure of *B. stearothermophilus* SpoIIAB have been determined and found to be distinct from Hank's type Ser protein kinases (41) while also exhibiting significant similarities to the ATPases of the Gyrase, Hsp90, Histidine kinase, and MutL superfamily (42). Similar to SpoIIAB and RsbW, the C-terminal region of PA3346 also has N, G1, and G2 boxes responsible for σ/anti-σ antagonist binding, Mg^{2+} ion binding, and ADP/ATP binding, respectively (43, 44) (Fig. 1).

PA3346C Is Divalent Cation-dependent Ser/Thr Protein Kinase—If PA3347 is an anti-σ factor antagonist, it is likely to be phosphorylated, and the phosphorylation should influence its interaction with the anti-σ factor. Phosphorylation of PA3347 at Ser-56 using the whole cell extract of *P. aeruginosa* PAO1 was demonstrated previously through an *in vitro* phosphorylation assay (12). The presence of a kinase domain at the C-terminal region of PA3346 implies that the protein is probably the kinase in PA3347 phosphorylation. To verify this possibility, the PA3346 C-terminal region ranging from nucleotide position 1222 to 1713 was cloned and overexpressed, and the recombinant protein, designated PA3346C, was used in the *in vitro* phosphorylation assay with [γ-^{32}P]ATP as a tracer. As shown in Fig. 2, PA3346C is capable of phosphorylating PA3347 but not PA3347-S56A, the PA3347 variant with an Ala substitution at Ser-56 (Fig. 2*A*). The PA3346C kinase activity was found to be dependent on the divalent cations Mg^{2+}, Ca^{2+}, and Mn^{2+} but not on Ni^{2+}, Co^{2+}, or Zn^{2+} (Fig. 2*B*). The kinetics study determined the K_m (0.645 ± 0.076 mM) and V_{max} (3.144 ± 0.148 mM/s) of PA3346C with PA3347 as the substrate (supplemental Fig. S1).

PA3346C Phosphorylates PA3347 at Ser-56—To further verify the phosphorylation site on PA3347, PA3347 with or without PA3346C treatment was subjected to trypsin digestion followed by MALDI-TOF mass spectrometry. The PA3347 sample treated with PA3346C and ATP yielded two peaks of 1849.997 and 1929.963 Da, respectively (supplemental Fig. S2A), representing unphosphorylated and phosphorylated Ser-56-containing peptides (NATYLDSSALGMLLLLR) of PA3347. However, the phosphorylated Ser-56-containing peptide peak of 1929.963 Da was not observed in the PA3347-S56A site-directed mutant (supplemental Fig. S2B). Together, the results indicate that PA3347 is phosphorylated at Ser-56 by PA3346C. The result is consistent with our previous finding using the whole cell extract to phosphorylate PA3347 (12).

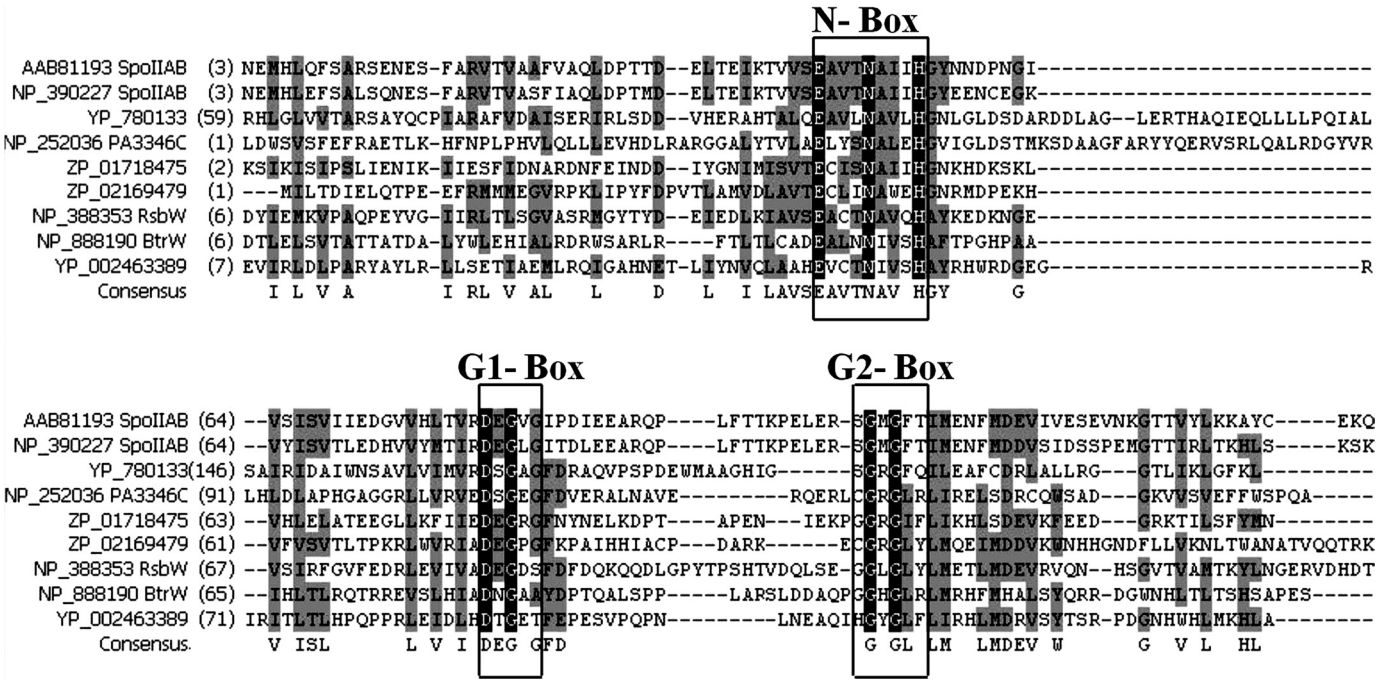

FIGURE 1. **Amino acid sequence alignment of PA3346C with other Ser/Thr protein kinases.** PA3346C (from Leu-408 to Ala-571) shows a 65% similarity and 26% identity to RsbW of *B. subtilis*, a 50% similarity and 28% identity to BtrW of *B. bronchiseptica*, and a 48% similarity and 32% identity to SpoIIAB of *B. subtilis*. Motifs labeled *N*, *G1*, and *G2*, which are commonly found in *histidine kinases/ATPases*, are indicated above the sequences. Amino acid residues with strong similarity are only considered in consensus sequences and are shaded in *gray*. The identical residues are shaded in *black*.

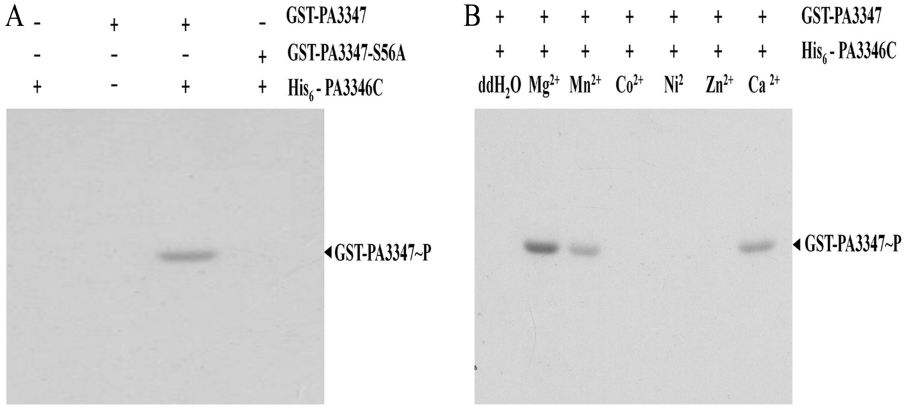

FIGURE 2. **PA3346C possesses divalent cation-dependent Ser/Thr protein kinase activity.** *A*, His_6-PA3346C was incubated with [γ-^{32}P]ATP in the presence of either GST-PA3347 or GST-PA3347-S56A. *B*, His_6-PA3346C and GST-PA3347 were incubated with [γ-^{32}P]ATP in the presence of different divalent cations. The proteins were resolved using SDS-PAGE and subjected to autoradiography. *ddH_2O*, double distilled H_2O.

PA3347 Interacts with PA3346C in Vitro—To function as an anti-σ antagonist, PA3347 must interact with PA3346C to perform regulatory activity. Using the GST pulldown assay, both PA3347 and PA3347-S56A were found to form a stable complex with PA3346C but only in the presence of ADP (Fig. 3*A*), suggesting that ADP stabilizes PA3346C in a conformation favorable for binding with PA3347 (Fig. 3*A*).

PA3347 Interacts with FlgM in Vitro—The *PA3347* deletion mutant MJL47 displayed a hyperswarming phenotype, suggesting an up-regulation of motility-related gene expression (12). In *P. aeruginosa* PAO1, the anti-σ factor FlgM-encoding gene (*PA3351*) is located immediately downstream of the *hptB-PA3346-PA3347* operon (12). Because FlgM has been shown to interact with the σ factor FliA (σ^{28}) to regulate the synthesis of flagella (17), this study examined whether PA3347 regulates the FliA-dependent flagellum activity by interacting with FlgM. As shown in Fig. 3*B*, the His_6-tagged FlgM could be co-eluted with either the GST-tagged PA3347 or the PA3347-S56A proteins, indicating an interaction between the FlgM protein and PA3347 or PA3347-S56A. Binding in the absence of ATP suggests that phosphorylation of PA3347 is not required for the interaction.

PA3347 Interacts with FlgM as Well as with PA3346C in Bimolecular Fluorescence Complementation Assay—To demonstrate that interaction of PA3347 with its binding partners FlgM and PA3346C is also taking place *in vivo*, a set of plasmids that are stable and express the proteins upon induction in *E. coli* BL21(DE3) was constructed for the BiFC assay. The cells harboring positive control plasmids gave a strong green fluorescence due to GFP reassembly, whereas negative control cells showed no green fluorescence. As shown in Fig. 4, cells harboring pNBIFC3347 and pCBIFC3351, expressing the NGFP-

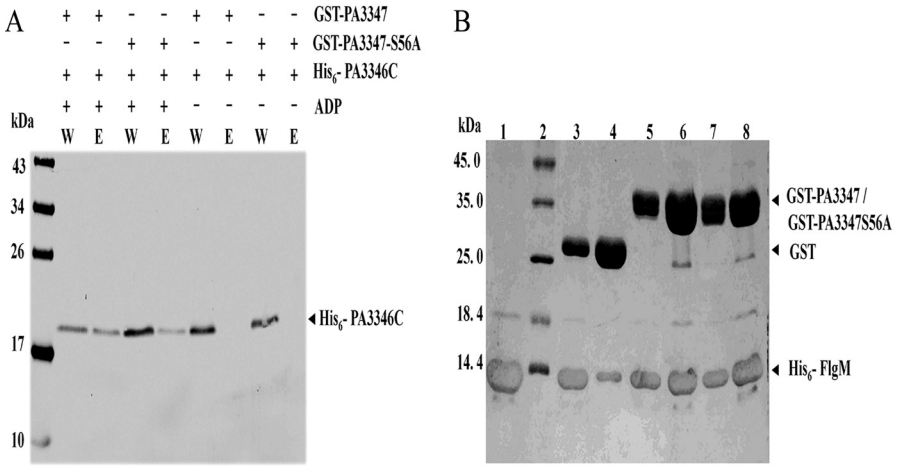

FIGURE 3. **Interaction of PA3347 with PA3346C and FlgM determined by GST pulldown assay.** *A*, PA3346C and PA3347 interact *in vitro*. The interaction of His_6-PA3346C with GST-PA3347 either in the presence or absence of ADP was determined by Western blot analysis. A monoclonal anti-His antibody was used to detect His_6-PA3346C in the eluted fraction of the GST pulldown assay. *W*, PBS wash fraction; *E*, fraction eluted with 20 mM glutathione. *B*, PA3347 and FlgM interact *in vitro*. The interaction between PA3347 and FlgM was monitored using affinity chromatography. Glutathione-Sepharose beads were incubated with affinity-purified GST-PA3347 and GST-PA3347-S56A with His_6-FlgM in a GST pulldown assay. GST was incubated with His_6-FlgM as a negative control. *Lane 1*, load amount of His_6-FlgM; *lane 2*, markers; *lane 3*, wash fraction from the negative control (GST and FlgM proteins); *lane 4*, eluted fraction from the negative control (GST and FlgM); *lane 5*, wash fraction from GST-PA3347 and His_6-FlgM; *lane 6*, eluted fraction from GST-PA3347 and His_6-FlgM; *lane 7*, wash fraction from GST-PA3347-S56A and His_6-FlgM; *lane 8*, eluted fraction from GST-PA3347-S56A and His_6-FlgM. Proteins were visualized on the gel using Coomassie Blue staining.

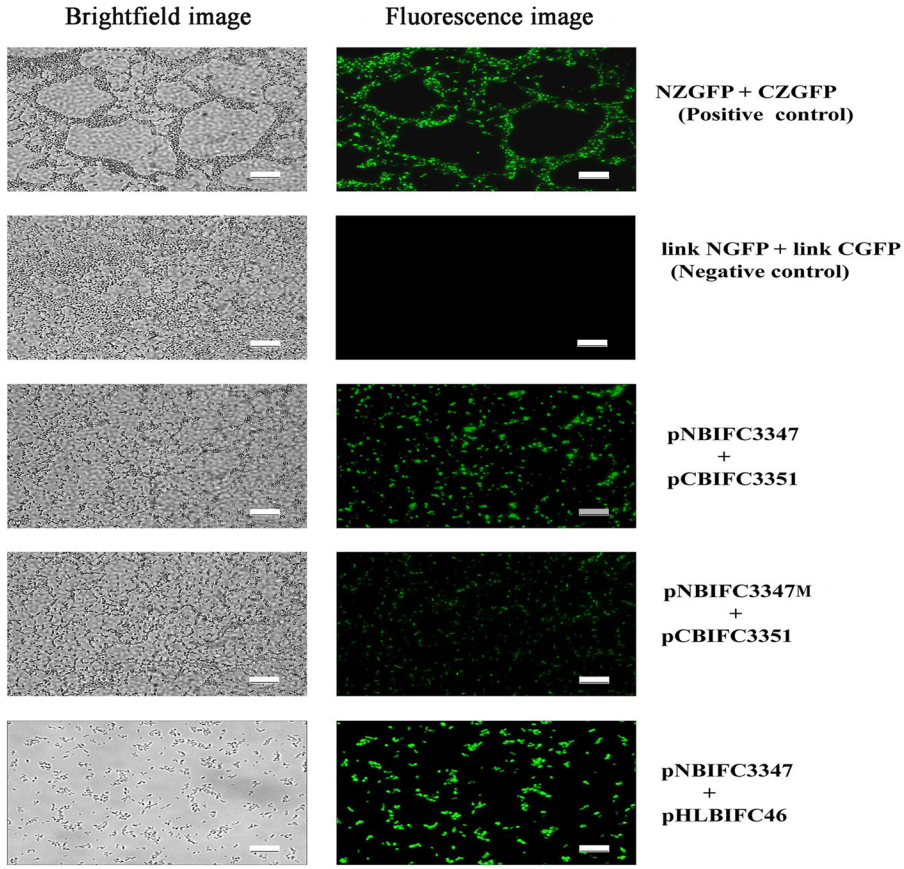

FIGURE 4. **Interaction of PA3347 with FlgM and PA3346C analyzed by bimolecular fluorescence complementation assay.** Bright field (*left*) and fluorescence (*right*) images of isopropyl β-D-thiogalactopyranoside- and arabinose-induced *E. coli* BL21(DE3) cells harboring the indicated plasmids taken at 600× *magnification* are shown. Cells co-expressing the leucine zipper peptide (positive control) displayed bright fluorescence emission, whereas no fluorescence was detected in the negative control cells. Fluorescence was detected in *E. coli* pNBIFC3347 + pCBIFC3351, *E. coli* pNBIFC3347M + pCBIFC3351, and *E. coli* pNBIFC3347 + pHLBIFC46, indicating a positive interaction in the following pairs: PA3347 and FlgM, PA3347-S56A and FlgM, and PA3347 and PA3346C. *Scale bar*, 15 μm.

PA3347 and CGFP-FlgM, respectively, exhibit green fluorescence, indicating an interaction of PA3347 and FlgM *in vivo*. A similar study also showed that PA3347-S56A can interact with FlgM. The result further indicates that phosphorylation is not required for PA3347 to interact with FlgM. Consistent with the *in vitro* protein-protein interaction results, *E. coli* BL21(DE3)

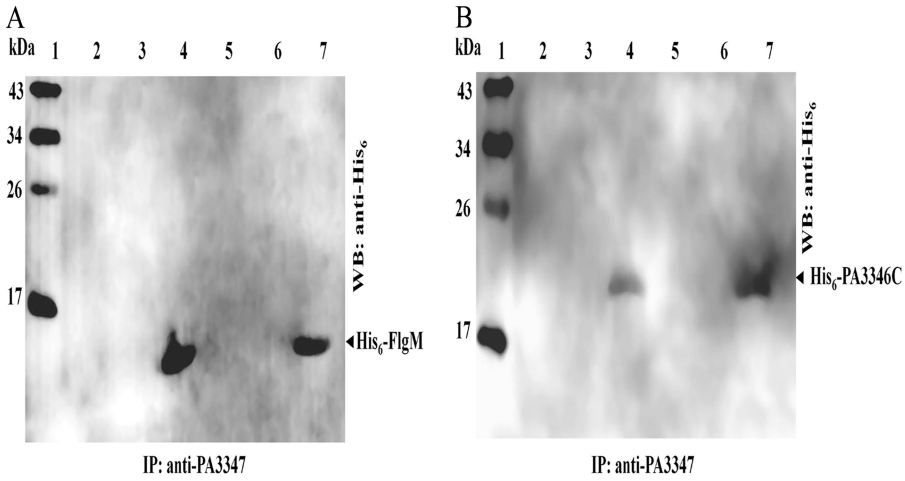

FIGURE 5. **PA3347 interacts with FlgM and PA3346C.** *A*, interaction between PA3347 and FlgM. *Lane 1*, molecular mass markers; *lane 2*, *P. aeruginosa* lysate; *lane 3*, His_6-FlgM; *lane 4*, *P. aeruginosa* lysate incubated with His_6-FlgM; *lane 5*, *E. coli* lysate expressing GST-PA3347-S56A; *lane 6*, His_6-FlgM; *lane 7*, *E. coli* lysate expressing GST-PA3347-S56A incubated with His_6-FlgM. *B*, interaction between PA3347 and PA3346C. *Lane 1*, molecular mass markers; *lane 2*, *P. aeruginosa* lysate; *lane 3*, His_6-PA3346C; *lane 4*, *P. aeruginosa* lysate incubated with His_6-PA3346C; *lane 5*, *E. coli* lysate expressing GST-PA3347-S56A; *lane 6*, His_6-PA3346C; *lane 7*, *E. coli* lysate expressing GST-PA3347-S56A incubated with His_6-PA3346C. *IP*, immunoprecipitation; *WB*, Western blot.

cells harboring pNBIFC3347 and pHLBIFC46, which encodes PA3346C, also showed green fluorescence (Fig. 4).

Co-immunoprecipitation of PA3347 with FlgM and PA3346C Proteins in Vivo—Co-immunoprecipitation analysis showed that recombinant His_6-FlgM and His_6-PA3346C proteins bound to both the PA3347 expressed in PAO1 and the recombinant GST-PA3347-S56A expressed in *E. coli*. A control experiment demonstrated that PA3347, PA3347-S56A, the antibody against PA3347, the recombinant His_6-FlgM, and His_6-PA3346C proteins alone do not bind to Protein A-Sepharose beads (Fig. 5, *A* and *B*).

Expression of Both fliA and flgM Is Regulated by PA3347—To determine whether PA3347 is involved in regulating the expression of *fliA* and *flgM*, we analyzed the expression of *flgM* and *fliA* in the presence and absence of PA3347. Compared with that of the wild type, the expression of *flgM* and *fliA* was significantly increased in PA3347 mutant MJL47 by ~5- and 13-fold, respectively, as determined by quantitative real time PCR. This is possibly because PA3347 deletion results in the partial loss of FlgM function as an anti-σ factor, which results in an increase of FliA activity to induce *fliA* and *flgM* transcription. It is necessary to mention only a partial loss because full loss of FlgM function would bring about uncontrolled filament assembly and loss of motility.

FliA Competes for Binding to FlgM-PA3347 Complex, and FlgM Competes for Binding to PA3347-PA3346C Complex—To verify that the HptB-PA3346-PA3347 signaling system can modulate flagellum activity through the interaction of FlgM and FliA, a GST pulldown competitive assay was performed. As shown in Fig. 6, increasing concentrations of FliA competitively displaced the binding of PA3347 to FlgM, demonstrating the well known finding that FliA interacts directly with the anti-σ factor FlgM (17).

Elucidation of whether PA3346C, FlgM, and PA3347 can form a stable complex or whether PA3346C and FlgM bind to PA3347 in a competitive manner is critical for understanding the regulatory mechanism exerted by the HptB-mediated signaling pathway. As shown in Fig. 7*A*, increasing concentrations

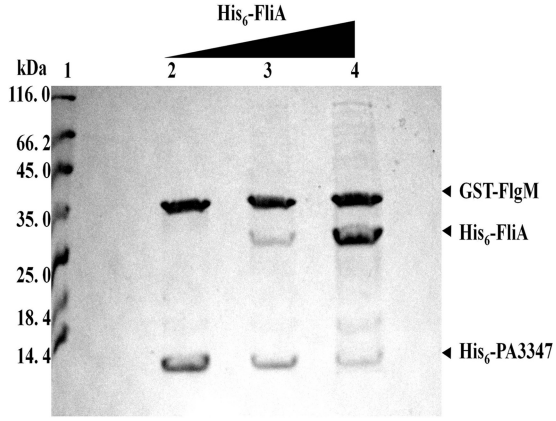

FIGURE 6. **FliA shows antagonist activity toward PA3347 in FlgM-PA3347 complex.** The competitive binding between His_6-FliA and His_6-PA3347 for immobilized GST-FlgM was carried out. The pulldown of GST-FlgM (30 μg/ml) was conducted in the presence of His_6-PA3347 (30 μg/ml) and increasing concentrations of His_6-FliA. *Lane 1*, markers; *lanes 2–4*, a constant concentration of GST-FlgM bound to His_6-PA3347 was incubated with increasing amounts of His_6-FliA (0, 20, 100 μg/ml, respectively). The proteins were resolved on an SDS-polyacrylamide gel and stained with Coomassie Blue.

of FlgM displaced the binding of PA3346C to PA3347 in the presence of ATP. However, displacement was not observed when ADP was used to replace ATP. This finding agrees with the expected partner-switching mechanism that the phosphorylation of the anti-σ antagonist by the Ser protein kinase in the presence of ATP could lead to the dissociation of the complexes, whereas ADP can stabilize the complexes (8, 9, 45). By contrast, the binding of FlgM to PA3347 was not affected by increasing concentrations of PA3346C in the presence of ATP or ADP. This suggests that the binding of FlgM and PA3347 is independent of the phosphorylation state (Fig. 7*B*).

PA3347 Phosphorylation Is Crucial for P. aeruginosa Swarming—Consistent with a previous finding (12), deleting *PA3347* increased the swarming motility, and the introduction of a plasmid that harbored a full-length *PA3347* (pMMB47) into MJL47 could reverse the hyperswarming motility to the parental phenotype (Fig. 8*A*). More interestingly, a plasmid

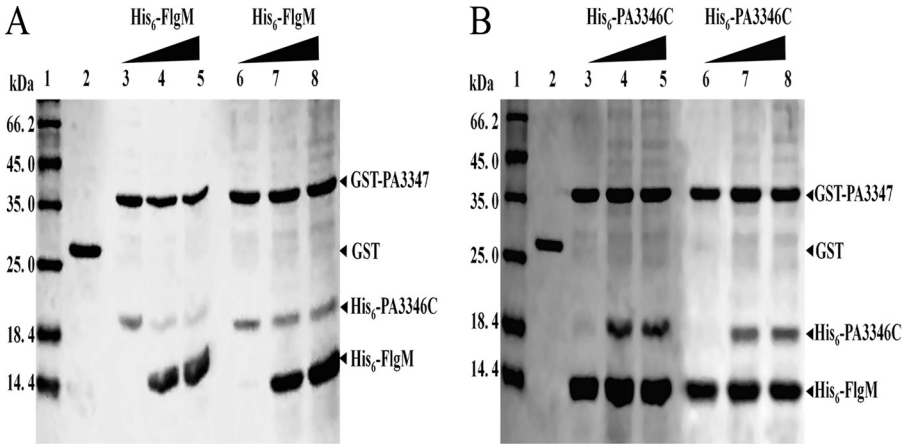

FIGURE 7. **Effect of PA3347 phosphorylation on binding to PA3346 and FlgM.** *A*, pulldown of GST-PA3347 (25 μg/ml) was performed in the presence of a constant concentration of His_6-PA3346C (30 μg/ml) and increasing concentrations of His_6-FlgM. *Lane 1*, markers; *lane 2*, the fraction eluted from the GST protein-immobilized column that was incubated with His_6-FlgM and His_6-PA3346C (negative control); *lanes 3–5*, His_6-PA3346C (30 μg/ml) bound to GST-PA3347 was incubated with increasing amounts of His_6-FlgM (0, 15, and 30 μg/ml, respectively) in the presence of 2 mM ATP and 2 mM $MgSO_4$; *lanes 6–8*, same as *lanes 3–5* except 2 mM ADP replaced ATP. *B*, pulldown of GST-PA3347 (25 μg/ml) was performed in the presence of His_6-FlgM (30 μg/ml) and increasing concentrations of His_6-PA3346C. *Lane 1*, molecular size markers; *lane 2*, eluted fraction from the GST protein-immobilized column that was incubated with His_6-FlgM and His_6-PA3346C (negative control); *lanes 3–5*, a constant concentration of His_6-FlgM bound to GST-PA3347 was incubated with increasing amounts of His_6-PA3346C (0, 10, and 20 μg/ml, respectively) in the presence of 2 mM ATP and 2 mM $MgSO_4$; *lanes 6–8*, same as *lanes 3–5* except 2 mM ADP replaced ATP. The proteins were resolved on an SDS-polyacrylamide gel and stained with Coomassie Blue.

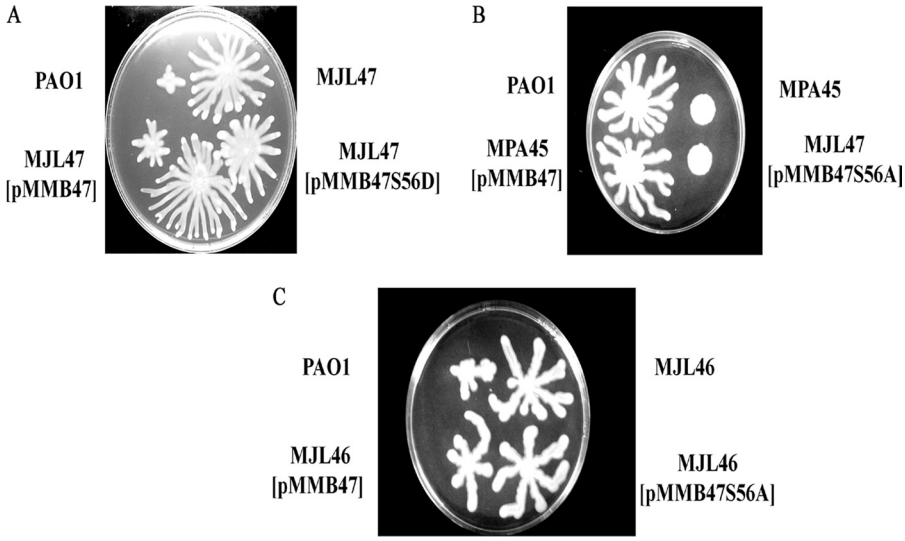

FIGURE 8. **Effects of amino acid substitution at Ser-56 of PA3347 on *P. aeruginosa* swarming.** Shown is the swarming motility of isogenic deletion mutants of *PA3347* (*A*), *hptB* (*B*), and *PA3346* (*C*) compared with the strains complemented with pMMB47, pMMB47S56A, and pMMB47S56D and the empty vector pMMB66EH in PAO1.

expressing a *PA3347* with an Asp substitution at Ser-56 (pMMB47S56D) to mimic a constitutively phosphorylated Ser residue can restore the hyperswarming activity of MJL47 to that of wild-type PAO1. By contrast, the plasmid pMMB47S56A producing a non-phosphorylated variant of *PA3347* cannot complement the hyperswarming phenotype of MJL47. Additionally, pMMB47 can restore the defect in the swarming phenotype of MPA45, whereas pMMB47S56A cannot (Fig. 8*B*). However, neither pMMB47 nor pMMB47S56A could complement the *PA3346* deletion mutant MJL46 to the parental phenotype (Fig. 8*C*). This suggests that the absence of the PA3346 as a kinase in MJL46 prevents the phosphorylation of *PA3347* produced from pMMB47 and hence formation of a stable complex with FlgM. These findings indicate that phosphorylation at Ser-56 of *PA3347* plays a critical role in regulating flagellum activity.

DISCUSSION

The objective of this study was to elucidate the molecular mechanism that leads to flagellum gene regulation by the HptB-PA3346-PA3347 signaling system in *P. aeruginosa* PAO1. The response regulator PA3346 differs from other transcriptional regulators because it is bifunctional, possessing both phosphatase and kinase activities. PA3346C was found to be a homolog of SpoIIAB. SpoIIAB performs the dual function of a Ser protein kinase and an anti-σ factor (46). This study has shown that PA3346C behaves like SpoIIAB, exhibiting a Ser protein kinase activity capable of phosphorylating PA3347 and an anti-σ antagonist binding activity.

This study also demonstrated a direct interaction between the anti-σ factor antagonist PA3347 and the anti-σ^{28} factor FlgM both *in vitro* and *in vivo*. The competition assay showed

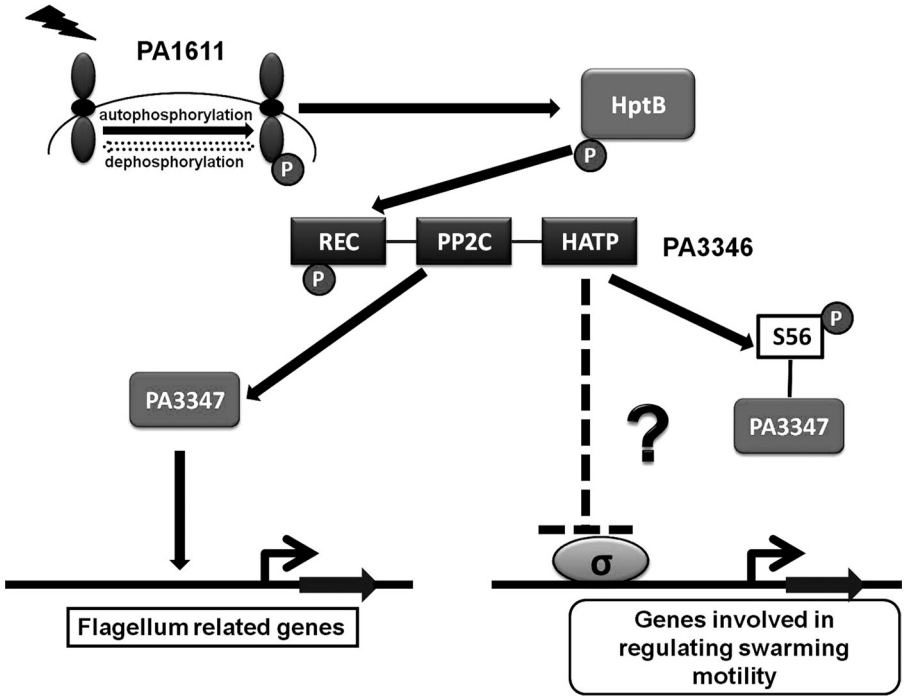

FIGURE 9. **Proposed model for PA3346–3347-FlgM partner-switching mechanism that regulates *P. aeruginosa* PAO1 swarming.** The N-terminal region of PA3346 can dephosphorylate PA3347. PA3347 binds FlgM, an anti-σ factor known to negatively regulate σ^{28} activity and affect flagellum structural biogenesis class III gene transcription. The C-terminal domain of PA3346, which is also known to act as a serine kinase, can phosphorylate PA3347, an anti-σ antagonist factor. The absence of PA3347 or the phosphorylation state of PA3347 can activate the PA3346 C terminus (shown as the *HATP* domain of PA3346 in the figure) to act as an anti-σ factor and inactivate the yet to be identified σ factor in a partner-switching mechanism. *REC*, receiver domain; *PP2C*, protein phosphatase 2C domain; *HATP*, histidine kinase/ATPase domain.

that the binding of FlgM to PA3347 was not affected by excess PA3346C, indicating that FlgM and PA3346C possibly use a different structural motif to interact with PA3347. However, the FlgM-PA3347 complex can be displaced by excess FliA, suggesting that both PA3347 and FliA may interact with FlgM possibly through the same binding site. Furthermore, the role of PA3347 phosphorylation in regulating swarming motility indicates that the regulation essentially occurs through a partner-switching mechanism. Partner-switching mechanisms for various Gram-positive bacteria have been documented. This type of regulation has been reported more recently for Gram-negative bacteria such as the Type III secretion system regulator BtrU-BtrW-BtrV in *B. bronchiseptica* (43). A conserved partner-switching regulatory system was also found in *Chlamydia trachomatis* (47). The partner-switching mechanism of *P. aeruginosa* may also have a widespread presence in related Gram-negative bacteria, controlling important aspects of bacterial physiology such as swarming.

According to the model established in this study (Fig. 9), HptB modifies the receiver domain of PA3346, altering the balance of phosphatase and kinase activity. In certain growth conditions, this alteration would affect flagellar gene expression through the partner-switching mechanism involving PA3347, FlgM, and FliA as demonstrated in this study. However, because swarming is a complex bacterial behavior, HptB may also affect swarming by other mechanisms. In analogy of SpoIIAB, the kinase domain of PA3346 (PA3346C) may act as an anti-σ factor to regulate a yet to be identified σ factor. This pathway may participate in cyclic di-GMP level modulation as suggested in a previous study (20, 48) and therefore may explain why the PA3347 deletion mutant shows a hyperswarming phenotype. In addition, this PA3346C-mediated pathway may affect the expression of genes unrelated to flagellum biogenesis that were found in our gene profiling analysis (supplemental Tables S2 and S3). Experiments are being carried out to verify these hypotheses.

Direct observation of the leading edge of the swarming colonies using optical microscopy showed that the wild-type colony edge exhibited vigorous and rapid collective cell movements. By contrast, cells at the leading edge of the *hptB* deletion MPA45 colony were resting (supplemental Videos S1 and S2). The absence of collective movement in the MPA45 strain, causing a defective swarming phenotype, is probably because the flagella were absent or incompletely assembled. To test this hypothesis, flagella were stained in both the wild-type and MPA45 swarming cells and examined under a microscope. Intriguingly, although both the microarray and real time PCR analyses showed that numerous flagellum regulatory and biosynthesis genes were significantly down-regulated in the *hptB* mutant, no apparent difference in the flagellum morphology was observed (supplemental Fig. S3, A and B). The *hptB* mutant cells even swarmed normally in broth with a chemical composition identical to the swarming agar. The twitching motility of the *hptB* mutant was also comparable with the wild-type cells, indicating normal type IV pili. Thus, the precise defects leading to the deficient swarming activity of the *hptB* mutant still require investigation. A component responsible for regulating rotation or supplying energy for flagellum movement is likely defective in the *hptB* mutant cells as also revealed by our gene expression profiling analysis. Such gene types have been

reported to affect the direction of flagellum motor rotation (49, 50) and the swarming motility in *Salmonella enterica* serovar Typhimurium (51).

REFERENCES

1. Mascher, T., Helmann, J. D., and Unden, G. (2006) Stimulus perception in bacterial signal-transducing histidine kinases. *Microbiol. Mol. Biol. Rev.* **70,** 910–938
2. Rodrigue, A., Quentin, Y., Lazdunski, A., Méjean, V., and Foglino, M. (2000) Two-component systems in *Pseudomonas aeruginosa*: why so many? *Trends Microbiol.* **8,** 498–504
3. Wyman, C., Rombel, I., North, A. K., Bustamante, C., and Kustu, S. (1997) Unusual oligomerization required for activity of NtrC, a bacterial enhancer-binding protein. *Science* **275,** 1658–1661
4. Da Re, S., Schumacher, J., Rousseau, P., Fourment, J., Ebel, C., and Kahn, D. (1999) Phosphorylation-induced dimerization of the FixJ receiver domain. *Mol. Microbiol.* **34,** 504–511
5. Francez-Charlot, A., Frunzke, J., Reichen, C., Ebneter, J. Z., Gourion, B., and Vorholt, J. A. (2009) σ factor mimicry involved in regulation of general stress response. *Proc. Natl. Acad. Sci. U.S.A.* **106,** 3467–3472
6. Alper, S., Duncan, L., and Losick, R. (1994) An adenosine nucleotide switch controlling the activity of a cell type-specific transcription factor in *B. subtilis*. *Cell* **77,** 195–205
7. Yang, X., Kang, C. M., Brody, M. S., and Price, C. W. (1996) Opposing pairs of serine protein kinases and phosphatases transmit signals of environmental stress to activate a bacterial transcription factor. *Genes Dev.* **10,** 2265–2275
8. Diederich, B., Wilkinson, J. F., Magnin, T., Najafi, M., Erringston, J., and Yudkin, M. D. (1994) Role of interactions between SpoIIAA and SpoIIAB in regulating cell-specific transcription factor σF of *Bacillus subtilis*. *Genes Dev.* **8,** 2653–2663
9. Kozak, N. A., Mattoo, S., Foreman-Wykert, A. K., Whitelegge, J. P., and Miller, J. F. (2005) Interactions between partner switcher orthologs BtrW and BtrV regulate type III secretion in *Bordetella*. *J. Bacteriol.* **187,** 5665–5676
10. Chen, Y. T., Chang, H. Y., Lu, C. L., and Peng, H. L. (2004) Evolutionary analysis of the two-component systems in *Pseudomonas aeruginosa* PAO1. *J. Mol. Evol.* **59,** 725–737
11. Lin, C. T., Huang, Y. J., Chu, P. H., Hsu, J. L., Huang, C. H., and Peng, H. L. (2006) Identification of an HptB-mediated multi-step phosphorelay in *Pseudomonas aeruginosa* PAO1. *Res. Microbiol.* **157,** 169–175
12. Hsu, J. L., Chen, H. C., Peng, H. L., and Chang, H. Y. (2008) Characterization of the histidine-containing phosphotransfer protein B-mediated multistep phosphorelay system in *Pseudomonas aeruginosa* PAO1. *J. Biol. Chem.* **283,** 9933–9944
13. Stover, C. K., Pham, X. Q., Erwin, A. L., Mizoguchi, S. D., Warrener, P., Hickey, M. J., Brinkman, F. S., Hufnagle, W. O., Kowalik, D. J., Lagrou, M., Garber, R. L., Goltry, L., Tolentino, E., Westbrock-Wadman, S., Yuan, Y., Brody, L. L., Coulter, S. N., Folger, K. R., Kas, A., Larbig, K., Lim, R., Smith, K., Spencer, D., Wong, G. K., Wu, Z., Paulsen, I. T., Reizer, J., Saier, M. H., Hancock, R. E., Lory, S., and Olson, M. V. (2000) Complete genome sequence of *Pseudomonas aeruginosa* PAO1, an opportunistic pathogen. *Nature* **406,** 959–964
14. Dasgupta, N., Wolfgang, M. C., Goodman, A. L., Arora, S. K., Jyot, J., Lory, S., and Ramphal, R. (2003) A four-tiered transcriptional regulatory circuit controls flagellar biogenesis in *Pseudomonas aeruginosa*. *Mol. Microbiol.* **50,** 809–824
15. Totten, P. A., Lara, J. C., and Lory, S. (1990) The rpoN gene product of *Pseudomonas aeruginosa* is required for expression of diverse genes, including the flagellin gene. *J. Bacteriol.* **172,** 389–396
16. Starnbach, M. N., and Lory, S. (1992) The fliA (rpoF) gene of *Pseudomonas aeruginosa* encodes an alternative σ factor required for flagellin synthesis. *Mol. Microbiol.* **6,** 459–469
17. Frisk, A., Jyot, J., Arora, S. K., and Ramphal, R. (2002) Identification and functional characterization of flgM, a gene encoding the anti-σ28 factor in *Pseudomonas aeruginosa*. *J. Bacteriol.* **184,** 1514–1521
18. Feldman, M., Bryan, R., Rajan, S., Scheffler, L., Brunnert, S., Tang, H., and Prince, A. (1998) Role of flagella in pathogenesis of *Pseudomonas aeruginosa* pulmonary infection. *Infect. Immun.* **66,** 43–51
19. Montie, T. C., Doyle-Huntzinger, D., Craven, R. C., and Holder, I. A. (1982) Loss of virulence associated with absence of flagellum in an isogenic mutant of *Pseudomonas aeruginosa* in the burned-mouse model. *Infect. Immun.* **38,** 1296–1298
20. Bordi, C., Lamy, M. C., Ventre, I., Termine, E., Hachani, A., Fillet, S., Roche, B., Bleves, S., Méjean, V., Lazdunski, A., and Filloux, A. (2010) Regulatory RNAs and the HptB/RetS signalling pathways fine-tune *Pseudomonas aeruginosa* pathogenesis. *Mol. Microbiol.* **76,** 1427–1443
21. Brencic, A., McFarland, K. A., McManus, H. R., Castang, S., Mogno, I., Dove, S. L., and Lory, S. (2009) The GacS/GacA signal transduction system of *Pseudomonas aeruginosa* acts exclusively through its control over the transcription of the RsmY and RsmZ regulatory small RNAs. *Mol. Microbiol.* **73,** 434–445
22. Smyth, G. K. (2004) Linear models and empirical Bayes methods for assessing differential expression in microarray experiments. *Stat. Appl. Genet. Mol. Biol.* **3,** Article3
23. Savli, H., Karadenizli, A., Kolayli, F., Gundes, S., Ozbek, U., and Vahaboglu, H. (2003) Expression stability of six housekeeping genes: a proposal for resistance gene quantification studies of *Pseudomonas aeruginosa* by real-time quantitative RT-PCR. *J. Med. Microbiol.* **52,** 403–408
24. Yuan, J. S., Reed, A., Chen, F., and Stewart, C. N., Jr. (2006) Statistical analysis of real-time PCR data. *BMC Bioinformatics* **7,** 85
25. Shevchenko, A., Wilm, M., Vorm, O., and Mann, M. (1996) Mass spectrometric sequencing of proteins silver-stained polyacrylamide gels. *Anal. Chem.* **68,** 850–858
26. Magliery, T. J., Wilson, C. G., Pan, W., Mishler, D., Ghosh, I., Hamilton, A. D., and Regan, L. (2005) Detecting protein-protein interactions with a green fluorescent protein fragment reassembly trap: scope and mechanism. *J. Am. Chem. Soc.* **127,** 146–157
27. Wilson, C. G., Magliery, T. J., and Regan, L. (2004) Detecting protein-protein interactions with GFP-fragment reassembly. *Nat. Methods* **1,** 255–262
28. Sanchez, C. J., Shivshankar, P., Stol, K., Trakhtenbroit, S., Sullam, P. M., Sauer, K., Hermans, P. W., and Orihuela, C. J. (2010) The pneumococcal serine-rich repeat protein is an intra-species bacterial adhesin that promotes bacterial aggregation *in vivo* and in biofilms. *PLoS Pathog.* **6,** e1001044
29. Shivshankar, P., Sanchez, C., Rose, L. F., and Orihuela, C. J. (2009) The *Streptococcus pneumoniae* adhesin PsrP binds to Keratin 10 on lung cells. *Mol. Microbiol.* **73,** 663–679
30. Beaton, A. R., Rodriguez, J., Reddy, Y. K., and Roy, P. (2002) The membrane trafficking protein calpactin forms a complex with bluetongue virus protein NS3 and mediates virus release. *Proc. Natl. Acad. Sci. U.S.A.* **99,** 13154–13159
31. Finelli, A., Gallant, C. V., Jarvi, K., and Burrows, L. L. (2003) Use of in-biofilm expression technology to identify genes involved in *Pseudomonas aeruginosa* biofilm development. *J. Bacteriol.* **185,** 2700–2710
32. Wilderman, P. J., Vasil, A. I., Johnson, Z., and Vasil, M. L. (2001) Genetic and biochemical analyses of a eukaryotic-like phospholipase D of *Pseudomonas aeruginosa* suggest horizontal acquisition and a role for persistence in a chronic pulmonary infection model. *Mol. Microbiol.* **39,** 291–303
33. Mukhopadhyay, S., Kapatral, V., Xu, W., and Chakrabarty, A. M. (1999) Characterization of a Hank's type serine/threonine kinase and serine/threonine phosphoprotein phosphatase in *Pseudomonas aeruginosa*. *J. Bacteriol.* **181,** 6615–6622
34. Martin, P. R., Hobbs, M., Free, P. D., Jeske, Y., and Mattick, J. S. (1993) Characterization of pilQ, a new gene required for the biogenesis of type 4 fimbriae in *Pseudomonas aeruginosa*. *Mol. Microbiol.* **9,** 857–868
35. Bren, A., and Eisenbach, M. (1998) The N terminus of the flagellar switch protein, FliM, is the binding domain for the chemotactic response regulator, CheY. *J. Mol. Biol.* **278,** 507–514
36. Toker, A. S., and Macnab, R. M. (1997) Distinct regions of bacterial flagellar switch protein FliM interact with FliG, FliN and CheY. *J. Mol. Biol.* **273,** 623–634
37. Arora, S. K., Ritchings, B. W., Almira, E. C., Lory, S., and Ramphal, R. (1998) The *Pseudomonas aeruginosa* flagellar cap protein, FliD, is respon-

sible for mucin adhesion. *Infect. Immun.* **66,** 1000–1007
38. Morey, J. S., Ryan, J. C., and Van Dolah, F. M. (2006) Microarray validation: factors influencing correlation between oligonucleotide microarrays and real-time PCR. *Biol. Proced. Online* **8,** 175–193
39. Campbell, E. A., Masuda, S., Sun, J. L., Muzzin, O., Olson, C. A., Wang, S., and Darst, S. A. (2002) Crystal structure of the *Bacillus stearothermophilus* anti-σfactor SpoIIAB with the sporulation σ factor σF. *Cell* **108,** 795–807
40. Min, K. T., Hilditch, C. M., Diederich, B., Errington, J., and Yudkin, M. D. (1993) σF, the first compartment-specific transcription factor of *B. subtilis*, is regulated by an anti-σ factor that is also a protein kinase. *Cell* **74,** 735–742
41. Zhang, C. C. (1996) Bacterial signalling involving eukaryotic-type protein kinases. *Mol. Microbiol.* **20,** 9–15
42. Dutta, R., and Inouye, M. (2000) GHKL, an emergent ATPase/kinase superfamily. *Trends Biochem. Sci.* **25,** 24–28
43. Mattoo, S., Yuk, M. H., Huang, L. L., and Miller, J. F. (2004) Regulation of type III secretion in *Bordetella*. *Mol. Microbiol.* **52,** 1201–1214
44. Garsin, D. A., Duncan, L., Paskowitz, D. M., and Losick, R. (1998) The kinase activity of the antiσ factor SpoIIAB is required for activation as well as inhibition of transcription factor σF during sporulation in *Bacillus subtilis*. *J. Mol. Biol.* **284,** 569–578
45. Cotter, P. A., and Miller, J. F. (1994) BvgAS-mediated signal transduction: analysis of phase-locked regulatory mutants of *Bordetella bronchiseptica* in a rabbit model. *Infect. Immun.* **62,** 3381–3390
46. Masuda, S., Murakami, K. S., Wang, S., Anders Olson, C., Donigian, J., Leon, F., Darst, S. A., and Campbell, E. A. (2004) Crystal structures of the ADP and ATP bound forms of the *Bacillus* anti-σ factor SpoIIAB in complex with the anti-anti-σ SpoIIAA. *J. Mol. Biol.* **340,** 941–956
47. Hua, L., Hefty, P. S., Lee, Y. J., Lee, Y. M., Stephens, R. S., and Price, C. W. (2006) Core of the partner switching signalling mechanism is conserved in the obligate intracellular pathogen *Chlamydia trachomatis*. *Mol. Microbiol.* **59,** 623–636
48. Petrova, O. E., and Sauer, K. (2011) SagS contributes to the motile-sessile switch and acts in concert with BfiSR to enable *Pseudomonas aeruginosa* biofilm formation. *J. Bacteriol.* **193,** 6614–6628
49. Alon, U., Camarena, L., Surette, M. G., Aguera y Arcas, B., Liu, Y., Leibler, S., and Stock, J. B. (1998) Response regulator output in bacterial chemotaxis. *EMBO J.* **17,** 4238–4248
50. Scharf, B. E., Fahrner, K. A., Turner, L., and Berg, H. C. (1998) Control of direction of flagellar rotation in bacterial chemotaxis. *Proc. Natl. Acad. Sci. U.S.A.* **95,** 201–206
51. Mariconda, S., Wang, Q., and Harshey, R. M. (2006) A mechanical role for the chemotaxis system in swarming motility. *Mol. Microbiol.* **60,** 1590–1602
52. Fürste, J. P., Pansegrau, W., Frank, R., Blöcker, H., Scholz, P., Bagdasarian, M., and Lanka, E. (1986) Molecular cloning of the plasmid RP4 primase region in a multi-host-range tacP expression vector. *Gene* **48,** 119–131